Journal of Applied and Computational Mechanics, Vol. 2, No. 4, (2016), 254-261

Journal of
Applied and Computational Mechanics

Dynamic buckling of embedded laminated nanocomposite plates based on sinusoidal shear deformation theory

Mohammd Sharif Zarei[1], Mohammad Hadi Hajmohammad[2,*], Ali Nouri[2]

[1]Faculty of Engineering, Ayatollah Boroujerdi University, Boroujerd, Iran
[2]Department of mechanical engineering, Imam hossein University, Tehran, Iran

Received December 2 2016; revised January 1 2017; accepted for publication January 2 2017.
Corresponding author: Mohammad Hadi Hajmohammad, hadi.hajmohammad@gmail.com

Abstract

In this study, dynamic buckling of embedded laminated nanocomposite plates is investigated. The plates are reinforced with single-walled carbon nanotubes (SWCNTs) where to obtain the equivalent material properties of them, Mori-Tanaka model is applied. Based on the sinusoidal shear deformation theory (SSDT), the motion equations are derived using energy method and Hamilton's principal. The Navier's method in conjunction with the Bolotin's method is used for obtaining the dynamic instability region (DIR) of the structure. The effects of different parameters such as volume percent of SWCNTs, number and orientation angle of layers, elastic medium and geometrical parameters of plates are shown on the DIR of the structure. Results indicate that increasing volume percent of SWCNTs increases the resonance frequency and shifts the DIR to right. Also, it is found that the present results have good agreement with previous researches.

Keywords: Dynamic buckling, Nanocomposite laminated plates, elastic medium, SSDT, Bolotin method.

1. Introduction

Stiff, strong and lightweight composite materials are being widely used in many structural members, such as multilayered composite plates. Laminated composite structures are made up of layers of orthotropic materials that are bonded together whereas sandwich structures consist of thick and light core surrounded by face sheets possessing high strength and high stiffness thereby increasing the resistance to bending. Dynamic stability problems which have attracted the attention of many researchers up to the present are among the most important problems for laminated composite plates even now.

There are many works for mechanical analysis of laminated plates. Natural frequencies and buckling stresses of cross-ply laminated composite plates were analyzed by Matsunaga [1] taking into account the effects of shear deformation, thickness change and rotatory inertia. The dynamic behavior of laminated composite plates undergoing moderately large deflection was investigated by Kim and Kim [2] considering the viscoelastic properties of the material. In order to accurately determine the dynamic response of cross-ply laminated thick plates subjected to moving load, a solution procedure based on the three-dimensional (3D) elasticity theory was presented by Malekzadeh et al. [3]. The Natural Neighbour Radial Point Interpolation Method (NNRPIM), an improved meshless method, was used by Dinis et al. [4] in the numerical implementation of an Unconstrained Third-Order Plate Theory applied to laminates. Honda et al. [5] extended the layerwise optimization (LO) procedure to the maximization problem of the fundamental frequencies of sandwich plates with fibrous composites and low stiffness core layers. A new Inverse Trigonometric Zigzag Theory was proposed by Sahoo and Singhand [6] implemented for the static

analysis of laminated composite and sandwich plates. Heydari et al. [7] studied an analytical approach for transverse bending analysis of an embedded symmetric laminated rectangular plate using Mindlin plate theory and the surrounding elastic medium simulated using Pasternak foundation. A simple hyperbolic shear deformation theory taking into account transverse shear deformation effects was proposed by Saidi et al. (8) for the free flexural vibration analysis of thick functionally graded plates resting on elastic foundations. A method to study dynamical instability and non-linear parametric vibrations of symmetrically laminated plates of complex shapes and having different cutouts was proposed by Awrejcewicz et al. [9]. Liang [10] extended the Koiter–Newton methodfor nonlinear buckling analysis of thick and thin laminated composite plates.

To the best of our knowledge, the dynamic buckling analyses of sandwich nanocomposite plates however have not received enough attentions so far. Motivated by these considerations, in order to optimize the sandwich structures, our end is to investigate dynamic buckling analysis of nanocomposite laminated plates resting on elastic medium based on SSDT. The elastic medium is simulated with orthotropic Pasternak medium. Navier and Bolotin methods are applied in order to obtain the DIR of system. To validate the work, the results are compared with those reported in the literature. The effects of different parameters such as volume percent of SWCNTs, number and orientation angle of layers, elastic medium and geometrical parameters of plates are shown on the DIR of the structure.

2. SSDT

A schematic figure of laminated plates with the nanocomposite layers is shown in Fig 1with the Cartesian coordinate system (x, y, z) which is taken in the middle layer of nano-composite where the thickness coordinate z ranges from $-h$ to $+h$. As can be seen in this figure, the length and width of the plates are *a* and *b*, respectively. The elastic medium is simulated by spring and shear layers.

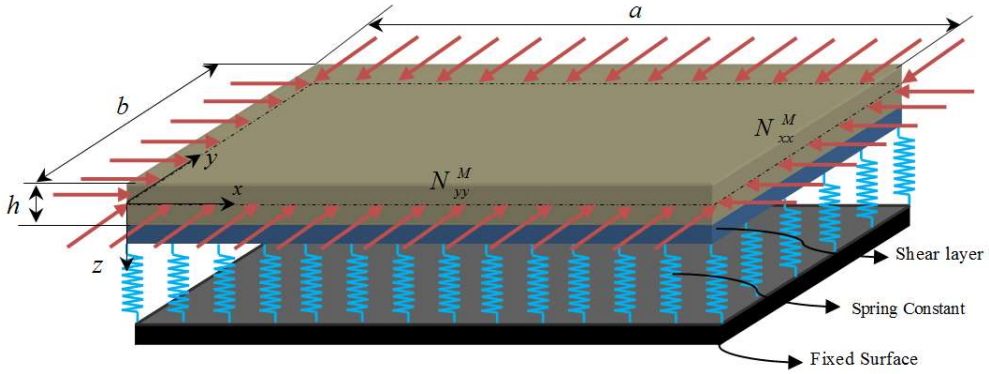

Fig. 1 The embedded laminated plate with SWCNTs-reinforced layers

Based on the SSDT, we have [11]

$$u_1(x,y,z,t) = u(x,y,t) - z\frac{\partial w}{\partial x} + \frac{2h}{\pi}\sin(\frac{\pi z}{2h})\varphi_x \ , \tag{1}$$

$$u_2(x,y,z,t) = v(x,y,t) - z\frac{\partial w}{\partial y} + \frac{2h}{\pi}\sin(\frac{\pi z}{2h})\varphi_y \ , \tag{2}$$

$$u_3(x,y,z,t) = w(x,y,t) + \cos(\frac{\pi z}{2h})\varphi(x,y,t) \ , \tag{3}$$

where u, v, and w are the displacements of the mid-plane along the axes x, y and z, respectively, and φ_x, φ_y and φ are the rotations about the y, x and z axes and account for the effect of transverse shear. According to the reference [38], further assumptions can be written as

$$w(x,y,t) = w_b(x,y,t) + w_s(x,y,t), \tag{4}$$

$$\varphi_x = \frac{\partial w_s}{\partial x}, \tag{5}$$

$$\varphi_y = \frac{\partial w_s}{\partial y}. \tag{6}$$

Based on displacement field of quasi-3D SSDPT, the in-plane and transverse shear strains of each layer may be expressed as

$$\varepsilon_{xx} = \frac{\partial u}{\partial x} + \frac{1}{2}(\frac{\partial w_b}{\partial x} + \frac{\partial w_s}{\partial x} + g(z)\frac{\partial \varphi}{\partial x})^2 - z\frac{\partial^2 w_b}{\partial x^2} - f(z)\frac{\partial^2 w_s}{\partial x^2}, \tag{7}$$

$$\varepsilon_{yy} = \frac{\partial v}{\partial y} + \frac{1}{2}(\frac{\partial w_b}{\partial y} + \frac{\partial w_s}{\partial y} + g(z)\frac{\partial \varphi}{\partial y})^2 - z\frac{\partial^2 w_b}{\partial y^2} - f(z)\frac{\partial^2 w_s}{\partial y^2}, \tag{8}$$

$$\varepsilon_{zz} = g'(\mathrm{z})\varphi, \tag{9}$$

$$\gamma_{xy} = \frac{\partial u}{\partial y} + \frac{\partial v}{\partial x} + \left(\frac{\partial w_b}{\partial x} + \frac{\partial w_s}{\partial x} + \mathrm{g(z)}\frac{\partial \varphi}{\partial x}\right)\left(\frac{\partial w_b}{\partial y} + \frac{\partial w_s}{\partial y} + \mathrm{g(z)}\frac{\partial \varphi}{\partial y}\right) - 2z\frac{\partial^2 w_b}{\partial y\,\partial x} - 2f\,(\mathrm{z})\frac{\partial^2 w_s}{\partial x^2}, \tag{10}$$

$$\gamma_{xz} = g\,(\mathrm{z})\left(\frac{\partial w_s}{\partial x} + \frac{\partial \varphi}{\partial x}\right), \tag{11}$$

$$\gamma_{yz} = g\,(\mathrm{z})\left(\frac{\partial w_s}{\partial y} + \frac{\partial \varphi}{\partial y}\right), \tag{12}$$

where $f\,(\mathrm{z}) = \mathrm{z} - \frac{h}{\pi}\sin\left(\frac{\pi z}{h}\right)$ and $g\,(\mathrm{z}) = \cos\left(\frac{\pi z}{h}\right)$.

The constitutive equation for stresses σ and strains ε matrix of the kth layer can be expressed as follows [12]

$$\begin{Bmatrix} \sigma_{xx} \\ \sigma_{yy} \\ \sigma_{xy} \\ \sigma_{xz} \\ \sigma_{yz} \end{Bmatrix}^{(\mathrm{k})} = \begin{bmatrix} Q_{11} & Q_{12} & Q_{16} & 0 & 0 \\ Q_{12} & Q_{22} & Q_{26} & 0 & 0 \\ Q_{16} & Q_{26} & Q_{66} & 0 & 0 \\ 0 & 0 & 0 & Q_{55} & Q_{45} \\ 0 & 0 & 0 & Q_{45} & Q_{44} \end{bmatrix}^{(\mathrm{k})} \begin{Bmatrix} \varepsilon_{xx} \\ \varepsilon_{yy} \\ \gamma_{xy} \\ \gamma_{xz} \\ \gamma_{yz} \end{Bmatrix}^{(\mathrm{k})}, \tag{13}$$

Where $Q_{ij}\ (i, j = 1,2,...,6)$ can be defined as

$$Q_{11} = C_{11}\cos^4\theta - 4C_{16}\cos^3\theta\sin\theta + 2\left(C_{12} + 2C_{66}\right)\cos^2\theta\sin^2\theta - 4C_{26}\cos\theta\sin^3\theta + C_{22}\sin^4\theta, \tag{14a}$$

$$Q_{12} = C_{12}\cos^4\theta + 2\left(C_{16} - C_{26}\right)\cos^3\theta\sin\theta + \left(C_{11} + C_{22} - 4C_{66}\right)\cos^2\theta\sin^2\theta + 2\left(C_{26} - C_{16}\right)\cos\theta\sin^3\theta + C_{12}\sin^4\theta, \tag{14b}$$

$$Q_{16} = C_{16}\cos^4\theta + \left(C_{11} - C_{12} - 2C_{66}\right)\cos^3\theta\sin\theta + 3\left(C_{26} - C_{16}\right)\cos^2\theta\sin^2\theta + \left(2C_{66} + C_{12} - C_{22}\right)\cos\theta\sin^3\theta - C_{26}\sin^4\theta, \tag{14c}$$

$$Q_{22} = C_{22}\cos^4\theta + 4C_{26}\cos^3\theta\sin\theta + 2\left(C_{12} + 2C_{66}\right)\cos^2\theta\sin^2\theta + 4C_{16}\cos\theta\sin^3\theta + C_{11}\sin^4\theta, \tag{14d}$$

$$Q_{26} = C_{26}\cos^4\theta + \left(C_{12} - C_{22} + 2C_{66}\right)\cos^3\theta\sin\theta + 3\left(C_{16} - C_{26}\right)\cos^2\theta\sin^2\theta + \left(C_{11} - C_{12} - 2C_{66}\right)\cos\theta\sin^3\theta - C_{16}\sin^4\theta, \tag{14e}$$

$$Q_{66} = 2\left(C_{16} - C_{26}\right)\cos^3\theta\sin\theta + \left(C_{11} + C_{22} - 2C_{12} - 2C_{66}\right)\cos^2\theta\sin^2\theta + 2\left(C_{26} - C_{26}\right)\cos\theta\sin^3\theta + C_{66}\left(\cos^4\theta + \sin^4\theta\right), \tag{14f}$$

$$Q_{44} = C_{44}\cos^2\theta + 2C_{45}\cos\theta\sin\theta + C_{55}\sin^2\theta, \tag{14g}$$

$$Q_{45} = \left(C_{55} - C_{44}\right)\cos\theta\sin\theta + C_{44}\left(\cos^2\theta - \sin^2\theta\right), \tag{14h}$$

$$Q_{55} = C_{55}\cos^2\theta - 2C_{45}\cos\theta\sin\theta + C_{44}\sin^2\theta, \tag{14i}$$

where θ denotes orientation angle and $C_{ij}\ (i, j = 1,2,...,6)$ are elastic coefficients which can be obtained by Mori-Tanaka model [13].

3. Energy Method

The strain energy, U of the structure can be written as

$$U = \frac{1}{2}\int_V \left(\sigma_{xx}^{(\mathrm{k})}\varepsilon_{xx} + \sigma_{yy}^{(\mathrm{k})}\varepsilon_{yy} + \sigma_{xy}^{(\mathrm{k})}\gamma_{xy} + \sigma_{xz}^{(\mathrm{k})}\gamma_{xz} + \sigma_{yz}^{(\mathrm{k})}\gamma_{yz}\right)dV. \tag{15}$$

Combining of Eqs. (7)-(13) yields

$$U=\frac{1}{2}\int_A\Big(N_x\frac{\partial u}{\partial x}+N_{xy}\frac{\partial u}{\partial y}+N_{xy}\frac{\partial v}{\partial x}+N_y\frac{\partial v}{\partial y}+Q_{xz}\frac{\partial w_s}{\partial x}+Q_{yz}\frac{\partial w_s}{\partial y}$$
$$+\left(S_x-M_x\right)\frac{\partial^2 w_s}{\partial x^2}+\left(S_y-M_y\right)\frac{\partial^2 w_s}{\partial y^2}+2\left(S_{xy}-M_{xy}\right)\frac{\partial^2 w_s}{\partial y\,\partial x}-M_x\frac{\partial^2 w_b}{\partial x^2}$$
$$-M_y\frac{\partial^2 w_b}{\partial y^2}-2M_{xy}\frac{\partial^2 w_b}{\partial y\,\partial x}+P_z\varphi+Q_{xz}\frac{\partial\varphi}{\partial x}+Q_{yz}\frac{\partial\varphi}{\partial y}\Big)dA, \tag{16}$$

where the force, moment and transverse shear stress resultants may be defined as

$$\left\{(N_x,N_y,N_{xy}),(M_x,M_y,M_{xy}),(S_x,S_y,S_{xy})\right\}=\sum_{k=1}^{N}\int_{z^{(k-1)}}^{z^{(k)}}\left\{\sigma_{xx},\sigma_{yy},\tau_{xy}\right\}(1,z,f)dz, \tag{17}$$

$$\left\{\left(Q_x,Q_y\right),\left(P_x,P_y\right)\right\}=\sum_{k=1}^{N}\int_{z^{(k-1)}}^{z^{(k)}}\left\{\sigma_{xz},\sigma_{yz}\right\}(g,f)dz, \tag{18}$$

The external work induced by the elastic medium is [14]:

$$W=-\frac{1}{2}\int\underbrace{\left(k_w w-k_g\nabla^2 \mathrm{w}\right)}_{q}wdA, \tag{19}$$

where k_w and k_g, respectively are spring and shear constants. The total kinetic energy of the actuator-nanocomposite-sensor structure may be written as

$$K=\frac{1}{2}\int_A\int_{-h/2}^{h/2}\rho^{(k)}\left(\left(u_1\right)^2+\left(u_2\right)^2+\left(u_3\right)^2\right)dzdA, \tag{20}$$

Based on Hamilton's principle, the motion equations can be derived as follows

$$\delta u:\ -\frac{\partial N_x}{\partial x}-\frac{\partial N_{xy}}{\partial y}+I_1\frac{\partial^2 u}{\partial t^2}-I_6\frac{\partial^3 w_b}{\partial x\,\partial t^2}+\left(I_7-I_6\right)\frac{\partial^3 w_s}{\partial x\,\partial t^2}=0, \tag{21}$$

$$\delta v:\ -\frac{\partial N_y}{\partial y}-\frac{\partial N_{xy}}{\partial x}+I_1\frac{\partial^2 v}{\partial t^2}-I_6\frac{\partial^3 w_b}{\partial y\,\partial t^2}+\left(I_7-I_6\right)\frac{\partial^3 w_s}{\partial y\,\partial t^2}=0, \tag{22}$$

$$\delta w_b:-\frac{\partial^2 M_x}{\partial x^2}-\frac{\partial^2 M_y}{\partial y^2}-2\frac{\partial^2 M_{xy}}{\partial y\,\partial x}+\Big[I_6\frac{\partial^3 u}{\partial x\,\partial t^2}+I_6\frac{\partial^3 v}{\partial y\,\partial t^2}+I_1\frac{\partial^2 w_b}{\partial t^2}+I_5\frac{\partial^2\varphi}{\partial t^2}$$
$$-N_{ye}\frac{\partial^2 w_b}{\partial y^2}-I_2\frac{\partial^4 w_b}{\partial x^2\partial t^2}-I_2\frac{\partial^4 w_b}{\partial y^2\partial t^2}+\left(I_8-I_2\right)\frac{\partial^4 w_s}{\partial x^2\partial t^2}-N_{xe}\frac{\partial^2 w_b}{\partial x^2}-N_{ye}\frac{\partial^2\varphi}{\partial y^2}$$
$$+\left(I_8-I_2\right)\frac{\partial^4 w_s}{\partial y^2\partial t^2}+I_1\frac{\partial^2 w_s}{\partial t^2}-N_{xe}\frac{\partial^2 w_s}{\partial x^2}-N_{ye}\frac{\partial^2 w_s}{\partial y^2}-N_{xe}\frac{\partial^2\varphi}{\partial x^2}+q=0, \tag{23}$$

$$\delta w_s:\ -\frac{\partial^2 M_x}{\partial x^2}-\frac{\partial^2 M_y}{\partial y^2}-2\frac{\partial^2 M_{xy}}{\partial y\,\partial x}+\frac{\partial^2 S_x}{\partial x^2}+\frac{\partial^2 S_y}{\partial y^2}+2\frac{\partial^2 S_{xy}}{\partial y\,\partial x}-\frac{\partial Q_{xz}}{\partial x}-\frac{\partial Q_{yz}}{\partial y}$$
$$+I_1\frac{\partial^2 w_b}{\partial t^2}+\left(I_2+I_8\right)\frac{\partial^4 w_b}{\partial x^2\partial t^2}+\left(I_3-I_2+2I_8\right)\frac{\partial^4 w_s}{\partial x^2\partial t^2}+\left(I_6+I_7\right)\frac{\partial^3 u}{\partial x\,\partial t^2}$$
$$+I_5\frac{\partial^2\varphi}{\partial t^2}+\left(I_3-I_2+2I_8\right)\frac{\partial^4 w_s}{\partial y^2\partial t^2}+\left(I_6+I_7\right)\frac{\partial^3 v}{\partial y\,\partial t^2}+I_1\frac{\partial^2 w_s}{\partial t^2}-N_{xe}\frac{\partial^2 w_b}{\partial x^2}-N_{ye}\frac{\partial^2\varphi}{\partial y^2}$$
$$-N_{xe}\frac{\partial^2\varphi}{\partial x^2}+\left(I_2+I_8\right)\frac{\partial^4 w_b}{\partial y^2\partial t^2}-N_{xe}\frac{\partial^2 w_s}{\partial x^2}-N_{ye}\frac{\partial^2 w_b}{\partial y^2}-N_{ye}\frac{\partial^2 w_s}{\partial y^2}+q=0, \tag{24}$$

$$\delta\varphi:\ P_z^l-\frac{\partial Q_{xz}}{\partial x}-\frac{\partial Q_{yz}}{\partial y}+I_4\frac{\partial^2\varphi}{\partial t^2}-N_{xe}\frac{\partial^2 w_b}{\partial x^2}-N_{xe}\frac{\partial^2 w_s}{\partial x^2}-N_{xe}\frac{\partial^2\varphi}{\partial x^2}+I_5\frac{\partial^2 w_s}{\partial t^2}$$
$$+I_5\frac{\partial^2 w_b}{\partial t^2}-N_{ye}\frac{\partial^2 w_b}{\partial y^2}-N_{ye}\frac{\partial^2 w_s}{\partial y^2}-N_{ye}\frac{\partial^2\varphi}{\partial y^2}=0, \tag{25}$$

where N_{xe} and N_{ye} are combination of mechanical, electrical and surface forces. Furthermore, the mass moments of inertia can be defined as

$$\left[I_1\ I_2\ I_3\ I_4\ I_5\ I_6\ I_7\ I_8\right]^{-1}=\sum_{k=1}^{N}\int_{z_{k-1}}^{z_k}\rho\ \left[1\ z\ z^2\ f\ f^2\ g\ g^2\ \mathrm{z}-f\ -zf\right]^{-1}dz, \tag{26}$$

4. Solution method

Steady state solutions to the governing equations of the plate motion which relate to the simply supported boundary conditions along the edges of the surface electrodes can be assumed as [15]

$$u(x,y)=u_0\cos\left(\frac{m\pi x}{a}\right)\sin\left(\frac{n\pi y}{b}\right), \tag{27}$$

$$v(x,y)=v_0\sin\left(\frac{m\pi x}{a}\right)\cos\left(\frac{n\pi y}{b}\right), \tag{28}$$

$$w_b(x,y)=w_{b0}\sin\left(\frac{m\pi x}{a}\right)\sin\left(\frac{n\pi y}{b}\right), \tag{29}$$

$$w_s(x,y)=w_{s0}\sin\left(\frac{m\pi x}{a}\right)\sin\left(\frac{n\pi y}{b}\right) \tag{30}$$

$$\varphi(x,y)=\varphi_0\sin\left(\frac{m\pi x}{a}\right)\cos\left(\frac{n\pi y}{b}\right), \tag{31}$$

Uniform compressive edge loading along x and y axis are $N_{xm}=-P$ and $N_{ym}=-kP$ respectively. Let the in-plane load P be periodic and may be expressed as

$$P(t)=\alpha P_{cr}+\beta P_{cr}\cos(\omega t), \tag{32}$$

where ω is the frequency of excitation, P_{cr} is the static buckling load, α and β may be defined as static and dynamic load factors, respectively. Now motion equations can be written as

$$\left\{[K-\alpha P_{cr}K_G-\beta P_{cr}\cos(\omega t)K_G][d]+[M][\ddot{d}]\right\}=[0], \tag{33}$$

where $[K]$ is the linear stiffness matrixes and $[M]$ is the mass matrix. In order to determinate the boundaries of dynamic instability regions, the method suggested by Bolotin [14] is applied. Hence, the components of $\{d\}$ can be written in the Fourier series with period $2T$ as

$$\{d\}=\sum_{k=1,3,\ldots}^{\infty}\left[\{a\}_k\sin\frac{k\omega t}{2}+\{b\}_k\cos\frac{k\omega t}{2}\right], \tag{34}$$

According to this method, the first instability region is usually the most important in studies of structures. It is due to the fact that the first DIR is wider that other DIRs and structural damping in higher regions becomes neutralize [4]. Substituting Eq. (34) into Eq. (33) and setting the coefficients of each sine and cosine as well as the sum of the constant terms to zero, yields

$$\left|\left([K]-P_{cr}\alpha[K_G]\pm P_{cr}\frac{\beta}{2}[K_G]-[M]\frac{\omega^2}{4}\right)\right|=0, \tag{35}$$

Solving the above equation based on eigenvalue problem, the variation of ω with respect to α can be plotted as DIR.

5. Numerical Results

A computer program is prepared for the numerical solution of dynamic buckling of laminated nano-composite plates resting on an elastic foundation. The material properties of laminated are listed in Table 1 [16].

Table 1 Material properties of Graphite/Epoxy [16]

Properties	Value
E_{11}	132.38 GPa
$E_{22}=E_{33}$	10.76 GPa
G_{12}	3.61 GPa
$G_{13}=G_{23}$	5.65 GPa
$\nu_{11}=\nu_{23}$	0.24
ν_{13}	0.49
ρ	1578 Kg/m^3

In the absence of similar publications in the literature covering the same scope of the problem, one cannot directly validate the results found here. However, the present work could be partially validated based on a simplified analysis suggested by Putcha and Reddy [17] on the buckling analysis of laminated plates for which the SWCNTS as reinforce and elastic medium in this paper were ignored ($k_w = k_g = C_r = 0$). For this purpose, a simply supported plate is considered with the material properties the same as Ref. [17]. The results of comparison are shown in Table 2. As can be seen, the present results are in good agreement with other works indication validation of this work.

Table 2 Comparison of present work with the published papers

Theory	E_1 / E_2				
	3	**10**	**20**	**30**	**40**
Classic theory, [17]	5.7538	11.4920	19.7120	27.9360	36.160
Mindlin theory, [17]	5.3991	9.9652	15.3510	19.7560	23.4530
Refined theory, [17]	5.3905	9.8336	14.8906	18.8778	22.1194
Present work	5.3918	9.8452	14.9167	18.8769	22.1531

Fig. 2 shows the effect of the number of layers on the DIR of the structure. It can be seen that in symmetric laminated composites (with three number of layers), the DIR occurs in higher pulsation frequencies compared with the anti-symmetric ones (with two number of layers). The reason is that the symmetric laminated composite plates are more balance and stable.

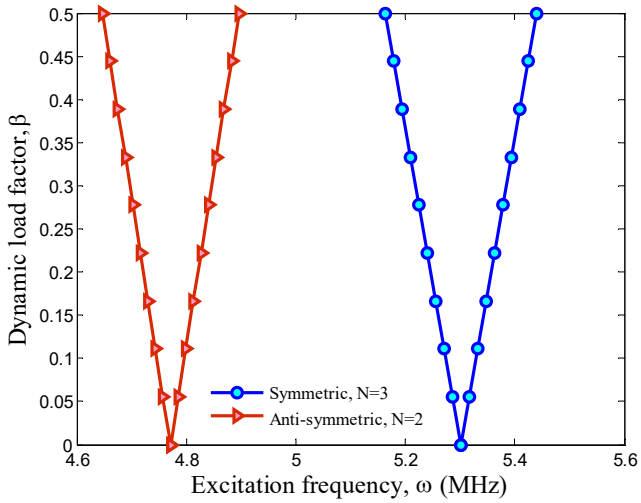

Fig 2 DIR of the structures with various number of layers

The influence of the orientation type of layers is studied in Fig 3. For this purpose, three various type of the orientation of layers are considered as: (0,0,0), (0,90,0) and (45,-45,45). According to Fig 3, it can be concluded that the composite structure with angle-ply orientation of layers has the highest frequency. Also the composite structure with zero angle of orientation has the lowest frequency and after that the structure with cross-ply orientation in layer.

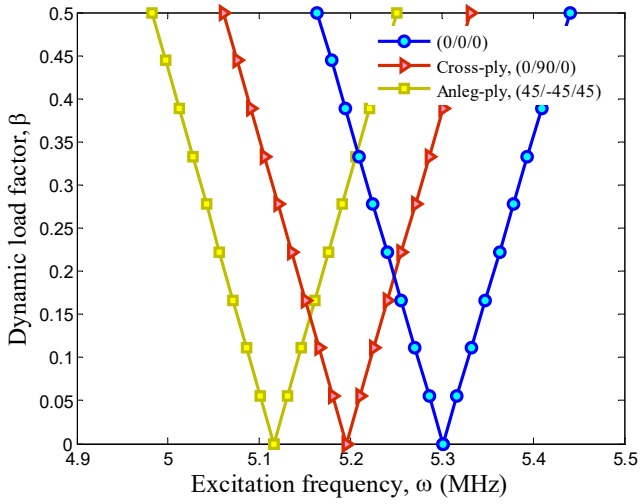

Fig 3 DIR of the structures with various types of orientation angle of layers

In Fig 4, the effect of the SWCNTs volume percent on the DIR is probed. From this figure it can be observed that with increasing the SWCNTs volume percent, the frequency increases and the DIR is happened in higher frequencies. Thereby, with increasing SWCNTs volume percent, the stiffness of the structure increases.

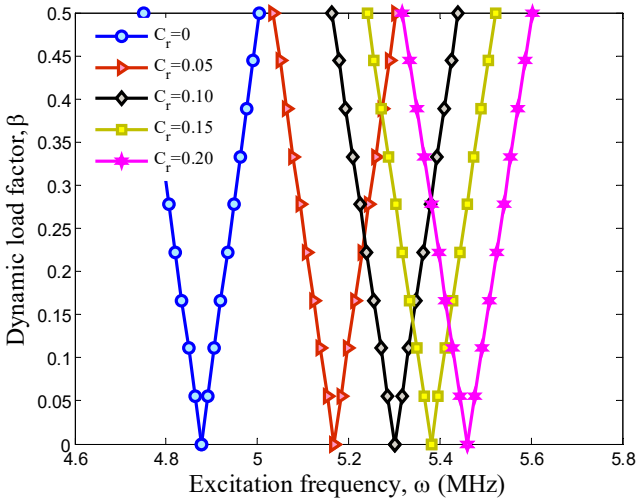

Fig 4 DIR of the structures with different values of SWCNTs volume percent versus axial mode number

The effect of the elastic medium which is modeled by the spring constant of Winkler medium and shear layer is studied in Fig 5. Generally the existence of the elastic medium causes to increase the stiffness of the structure and thereby the frequency increases. The Pasternak medium considers the vertical and shear loads however the Winkler medium considers only the vertical ones, therefore the effect of Pasternak medium is more than Winkler medium. According to Fig 5, the effect of the elastic medium on the DIR is significant and it can be a useful parameter to take away the system from dynamic buckling condition.

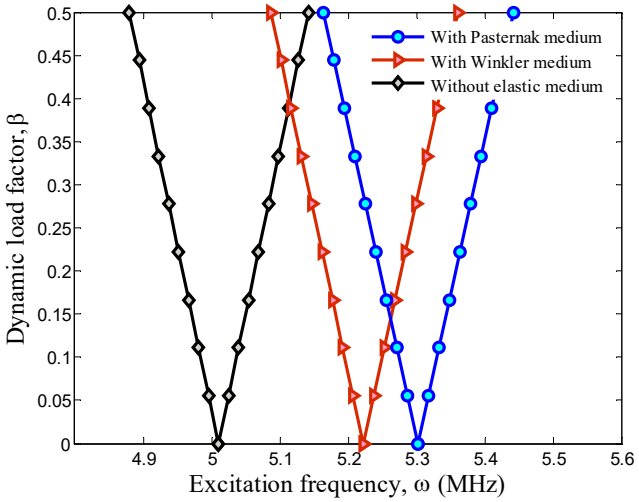

Fig 5 The effect of the elastic medium on the DIR of the structure

Fig 6 examines the influence of the loading types on the DIR of the structure. Two types of loading include uniaxial (along the *x* axis) and biaxial (along the *x* and *y* axes) are considered. As it can be found, in biaxial loading type the frequency is lower than axial loading type. The reason is that, in biaxial loading type, the load which applied to the edges is higher than the axial loading type and therefore the DIR of the structure occurs sooner.

6. Conclusion

Based on SSDT, dynamic buckling analysis of an embedded laminated nanocomposite plate was studied in this paper. The structure was surrounded by an elastic medium which generally was simulated by Pasternak foundation. Using energy method and Hamilton's principle, the motion equations were derived. In order to obtain the DIR, Navier and Bolotin methods were performed. The effects of elastic medium, volume percent of SWCNTs, number of layers and geometrical parameters of plate on the DIR of the structure were considered. Results indicate that considering elastic medium increases frequency of the plate. Also, increasing the volume percent of SWCNTs increases the frequency of the plate and DIR happens in higher frequencies. In addition, present results are in a good agreement with those reported by Ref. [17]. Finally, it is hoped that the results presented in this paper would be

helpful for study and design of rectangular laminated nanocomposite plates.

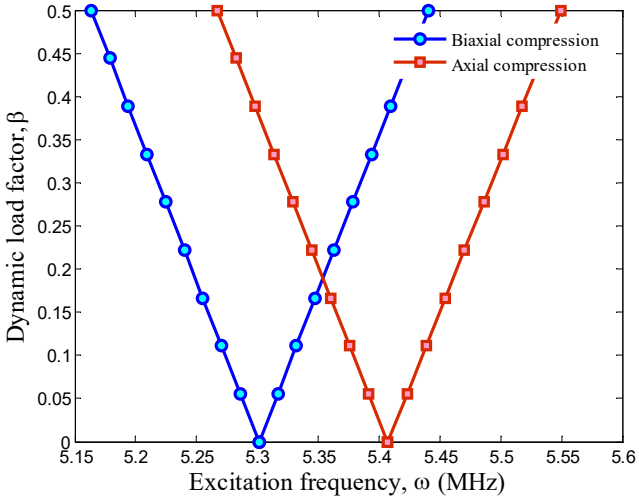

Fig 6 The effect of the loading type on the DIR of the structure

References

[1] Matsunag, H., "Vibration and stability of cross-ply laminated composite plates according to a global higher-order plate theory", Composite Structures, Vol. 48, pp. 231-244, 2000.
[2] Kim, T.W. and Kim, J.H., "Nonlinear vibration of viscoelastic laminated composite plates", International Journal of Solids and Structures, Vol. 39, pp. 2857–2870, 2002.
[3] Malekzadeh, P., Fiouz, A.R. and Razi, H., "Three-dimensional dynamic analysis of laminated composite plates sujected to moving load", Composite Structures, Vol. 90, pp. 105–114, 2009.
[4] Dinis, L.M.J.S., Natal Jorge, R.M. and Belinha, J., "Static and dynamic analysis of laminated plates based on an unconstrained third order theory and using a radial point interpolator meshless method", Computers and Structures, Vol. 89, pp. 1771–1784, 2011.
[5] Honda, Sh., Kumagai, T., Tomihashi, K. and Narita, Y., "Frequency maximization of laminated sandwich plates under general boundary conditions using layerwise optimization method with refined zigzag theory", Journal of Sound and Vibration, Vol. 332, pp. 6451–6462, 2013.
[6] Sahoo, R. and Singh, B.N., "A new shear deformation theory for the static analysis of laminated composite and sandwich plates", International Journal of Mechanical Sciences, Vol. 75, pp. 324–336, 2013.
[7] Heydari, M.M., Kolahchi, R., Heydari, M. and Abbasi, A., "Exact solution for transverse bending analysis of embedded laminated Mindlin plate", Structural Engineering and Mechanics, Vol. 49(5), pp. 661–672, 2014.
[8] Saidi, H., Tounsi, A. and Bousahla, A.A., "A simple hyperbolic shear deformation theory for vibration analysis of thick functionally graded rectangular plates resting on elastic foundations", Geomechanics and Engineering, Vol. 11, pp. 289-307, 2016.
[9] Awrejcewicz, J., Kurpa, L. and Mazur, O., "Dynamical instability of laminated plates with external cutout", International Journal of Non-Linear Mechanics, Vol. 81, pp. 103–114, 2016.
[10] Liang, K., "Koiter–Newton analysis of thick and thin laminated composite plates using a robust shell element", Composite Structures, Vol. 161, pp. 530-539, 2017.
[11] Thai, H.T. and Kim, S.E., "A simple quasi-3D sinusoidal shear deformation theory for functionally graded plates", Composite Structures, Vol. 99, pp. 172-178, 2013.
[12] Reddy, J.N., "A Simple Higher Order Theory for Laminated Composite Plates", Journal of Applied Mechanics, Vol. 51, pp. 745–752, 1984.
[13] Shi, D.L.and Feng, X.Q., "The Effect of Nanotube Waviness and Agglomeration on the elastic Property of Carbon Nanotube-Reinforced Composties", Journal of Engineering Materials and Technology, Vol. 126, pp. 250-270, 2004.
[14] Kolahchi, R., Safari, M. and Esmailpour, M., "Dynamic stability analysis of temperature-dependent functionally graded CNT-reinforced visco-plates resting on orthotropic elastomeric medium", Composite Structures, Vol. 150, pp. 255-265, 2016.
[15] Akhavan, H., Hosseini Hashemi, Sh., Rokni Damavandi Taher, H., Alibeigloo, A. and Vahabi, Sh., "Exact solutions for rectangular Mindlin plates under in-plane loads resting on Pasternak elastic foundation. Part I: Buckling analysis", Computational Material and Science, Vol. 44, pp. 968–978, 2009.
[16] Phung-Van, P., De Lorenzis, L., Thai, Ch.H., Abdel-Wahab, M. and Nguyen-Xuan, H., "Analysis of laminated composite plates integrated with piezoelectric sensors and actuators using higher-order shear deformation theory and isogeometric finite elements", Computational Material and Science, Vol. 96, pp. 495–505, 2015.
[17] Putcha, N.S. and Reddy, J.N., "Stability and natural vibration analysis of laminated plates by using a mixed element based on a refined plate theory", Journal of Sound and Vibration, Vol. 104, pp. 285–300, 1986.